# TR 3.1

# MIMO CHANNEL MODELS

# Contents

***Abstract –MIMO (Multiple-In Multiple-Out) mechanisms allow for increased diversity or data rate as compared to a communications system with single transmitting and receiving antenna. Multiple antenna schemes are not currently widely utilized for broadcasting. Therefore, not many realistic channel models are available. As suitable MIMO schemes for broadcasting need to be studied for DVB-NGH system, common channel model is necessary. In this document, such channel model for cross-polar MIMO is presented. In addition to the channel model, the measurement process for generating the models is described.***

# 1 INTRODUCTION

In this report the MIMO (Multiple-Input Multiple-Output) channel models created for DVB-NGH system design are presented. The channel model is generated based on field measurements. This report consists of three main parts, definition of the signal used for the measurements, the measurement campaign report and the resulting channel model description.

The measured signal is based the OFDM format of DVB-T. The first transmitter radiates DVB-T scattered pilots, continual pilots and TPS pilots exactly as defined in [1]. Since 2-transmitter MIMO channel measurement is required, modifications to the signal for the second transmitter are necessary. These are as follows: on every other OFDM symbol, the sign of the scattered pilots is reversed (i.e. the pilot is inverted) with respect to that defined in [1].

A high-power 2-by-2 cross-polar MIMO channel sounding campaign was carried out in the city of Helsinki, Finland, as part of the DVB-NGH MIMO investigation. This was carried out in collaboration with BBC, Digita, Elektrobit, Nokia, Tampere University and Turku University of Applied Sciences (TUAS) which are involved with the Celtic ENGINES project.

The cross-polar channel models that have been created on the basis of the measurements are presented in this document. The target is to give common definitions of channel models for all who will use them in simulations and laboratory measurements. A variety of models are included to cover a wide range of reception conditions. Also specific channel definitions for testing receiver synchronization issues in SFN-conditions are included.

# 2 MEASUREMENT SIGNAL DEFINITION

The proposed signal is based the OFDM format of DVB-T. This signal is defined in [1] and features a 1-in-12 pilot structure intended for channel estimation. The first transmitter radiates DVB-T scattered pilots, continual pilots and TPS pilots exactly as defined in [1]. Since 2-transmitter MIMO channel measurement is required, modifications to the signal for the second transmitter are necessary. These are as follows: on every other OFDM symbol, the sign of the scattered pilots is reversed (i.e. the pilot is inverted) with respect to that defined in [1]. In addition, continual pilots which lie on carriers which at times coincide with an inverted pilot are permanently inverted to allow consistency when they are indeed coincident.

TPS data is arbitrary as it is not anticipated it will be used in the channel measurement applications.

The data cells are assigned fixed BPSK data obtained from the DVB-T reference sequence of [1] para. 4.5.2.

## 2.1 Signal definition

### 2.1.1 OFDM frame structure

OFDM frame structure shall be as reference [1] paragraph 4.4 with the following changes/exceptions:

2k mode only
8MHz channel only

### 2.1.2 Reference signals

#### Location of scattered pilots

Reference information, taken from the reference sequence of [1] para. 4.5.2, is transmitted in scattered pilot cells in every symbol. Scattered pilot cells are always transmitted at the "boosted" power level of 16/9 relative to data bearing carriers. Thus the corresponding modulation is given by:

$$\mathrm{Re}\{c_{m,l,k}\} = \frac{4}{3} \times 2\left(\frac{1}{2} - w_k\right)$$

$$\mathrm{Im}\{c_{m,l,k}\} = 0$$

where $m$ is the frame index, $k$ is the frequency index of the carriers and $l$ is the time index of the symbols.

For the symbol of index $l$ ($l$ ranging from 0 to 67), carriers for which index $k$ belongs to the subset $k = K_{min} + 3 \times (l \bmod 4) + 12p$ ($p$ integer, $p \geq 0$, $k$ in range $[K_{min}; K_{max}]$) are scattered pilots.
The pilot insertion pattern is shown in figure 11 of [1] 4.5.3.

#### Location and modulation of continual pilots

In addition to the scattered pilots, 45 locations for continual1 pilots are defined in [1] para. 4.5.4 for 2k mode.

All continual pilots are modulated according to the reference sequence, see ref. [1] para. 4.5.2.

The continual pilots are transmitted at "boosted" power level.

Thus the corresponding modulation is given by, on transmitter 1 of 2:

$$\mathrm{Re}\{c_{m,l,k}\} = \frac{4}{3} \times 2\left(\frac{1}{2} - w_k\right)$$

$$\mathrm{Im}\{c_{m,l,k}\} = 0$$

#### Modification to pilots on transmitter 2

Transmitter 2 has scattered pilots inverted every other OFDM symbol to allow for MIMO channel measurement. Continual pilots falling on scattered-pilot-bearing carriers are inverted compared to transmitter 1 if the coincident scattered pilot is inverted; continual pilots without this property are not inverted.

Scattered pilots on transmitter 2:

$$\mathrm{Re}\{c_{m,l,k}\} = \frac{4}{3} \times (-1)^l \times 2\left(\frac{1}{2} - w_k\right) \quad \text{(symbol no. } l \text{ in the range } 0\ldots67)$$

$$\mathrm{Im}\{c_{m,l,k}\} = 0$$

Continual pilots on transmitter 2:

$$\mathrm{Re}\{c_{m,l,k}\} = \frac{4}{3} \times (-1)^l \times 2\left(\frac{1}{2} - w_k\right) \text{ if } k \bmod 3 = 0$$

$$\mathrm{Re}\{c_{m,l,k}\} = \frac{4}{3} \times 2\left(\frac{1}{2} - w_k\right) \text{otherwise}$$

$$\mathrm{Im}\{c_{m,l,k}\} = 0$$

#### Amplitudes of all reference information

Reference [1] para 4.5.5 shall apply.

### 2.1.3 TPS pilots

This is defined in accordance with [1] para. 4.6, 2k mode, but may have arbitrary information in $s_0$- $s_{67}$.

### 2.1.4 Data carriers

#### Location and modulation of the data carriers

The set of data carriers associated with the $l^{th}$ symbol of the $m^{th}$ transmission frame has 1512 elements and is denoted here by $\{data\ carriers\}_{m,l}$. It is the complement of the set of reference and TPS carriers, and we shall index it with $v$ in the range (0….1511)

*Transmitter* 1*:*
Data carriers depend only on the indices $v$ and $l$ and are given by

$$\mathrm{Re}\{c^{(1)}_{m,l,v}\} = 2\left(\frac{1}{2} - d_{v,l}\right) \text{ for } v \in \{0\ldots1511\} \text{ and } l \in \{0\ldots67\}$$

$$\mathrm{Im}\{c_{m,l,v}\} = 0$$

with $d_{v,l}$, as specified in the following section.

*Transmitter 2*:
Data carriers depend on the indices $v$ and $l$ and are given by

$$\mathrm{Re}\left\{c^{(2)}_{m,l,v}\right\} = (-1)^l \times 2\left(\frac{1}{2} - d_{v,l}\right) \text{ for } v \in \{0\ldots1511\} \text{ and } l \in \{0\ldots67\}$$

$$\mathrm{Im}\left\{c_{m,l,v}\right\} = 0$$

with $d_{v,l}$, as specified in the following section.

## PRBS sequence of the data carriers

The data carriers are modulated according to a different PRBS sequence, $d_{v,l}$ corresponding to their respective data carrier index $v$ and the frame index $l$. This PRBS sequence with its initialization sequence is shown in the diagram below.

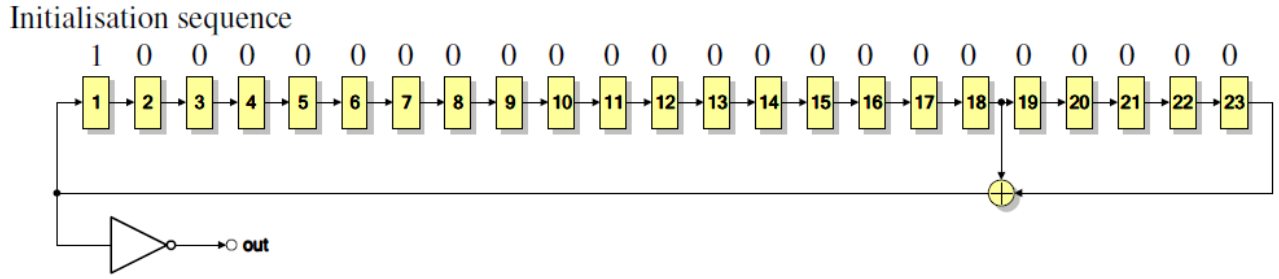


The PRBS is initialised so that the first output bit from the PRBS coincides with the first active carrier (data or signalling) of the first OFDM symbol in the frame, i.e. $l$=0. Subsequent bits from the sequence are mapped in order to the active carriers in the remaining symbols in the frame $l$=1 to $l$=67. However if the carrier is not a data carrier, the PRBS output is discarded. In this way, within the $l^{th}$ symbol, 1705 bits are generated by the PRBS but only 1512 are used corresponding to $v$ in the range 0…1511.

So if the sequence is $u_m$ with $m \in 0\ldots(1705^* 68) - 1$ then we can write (as pseudocode)

```
F=68;
P=1705;
for l=0:F-1
    v=0;
    for p=0:P-1
        if carrier==data_carrier
            d(v,l)=u(p+l*P);
            v=v+1;
        end
    end
end
```

The The PRBS will be re-initialised at the start of every OFDM frame.

The polynomial for the PRBS generator for data carriers is $X^{23} + X^{18} + 1$, as specified by ITU-T recommendation O.151, clause 2.2.

# 3 MEASUREMENT CAMPAIGN

A high-power 2-by-2 cross-polar MIMO channel sounding campaign was carried out in the city of Helsinki, Finland, as part of the DVB-NGH MIMO investigation. This was carried out in collaboration with BBC, Digita, Elektrobit, Nokia, Tampere University and Turku University of Applied Sciences (TUAS) which are

involved with the Celtic ENGINES project. Amphenol has kindly assist in the sounding by providing an application antenna. The channel sounding campaign was scheduled for 5 days starting from Monday the 28th of June 2010. The data collected from the measurement campaign will be processed to obtain a realistic 2-by-2 cross-polar MIMO channel model to be used in simulation for technical proposal evaluation.

## 3.1 Locations

The channel data was recorded in 4 different locations:

1. Digita office (indoor and outdoor)
2. Outdoor measurement at the Helsinki Olympic stadium car park (outdoor)
3. Tekes office (indoor and outdoor walkway)
4. High power non-line-of-sight outdoor (near Pasila Tower / Tekes office)

These locations are indicated in Figure 1 below along with the location of the transmitting tower.

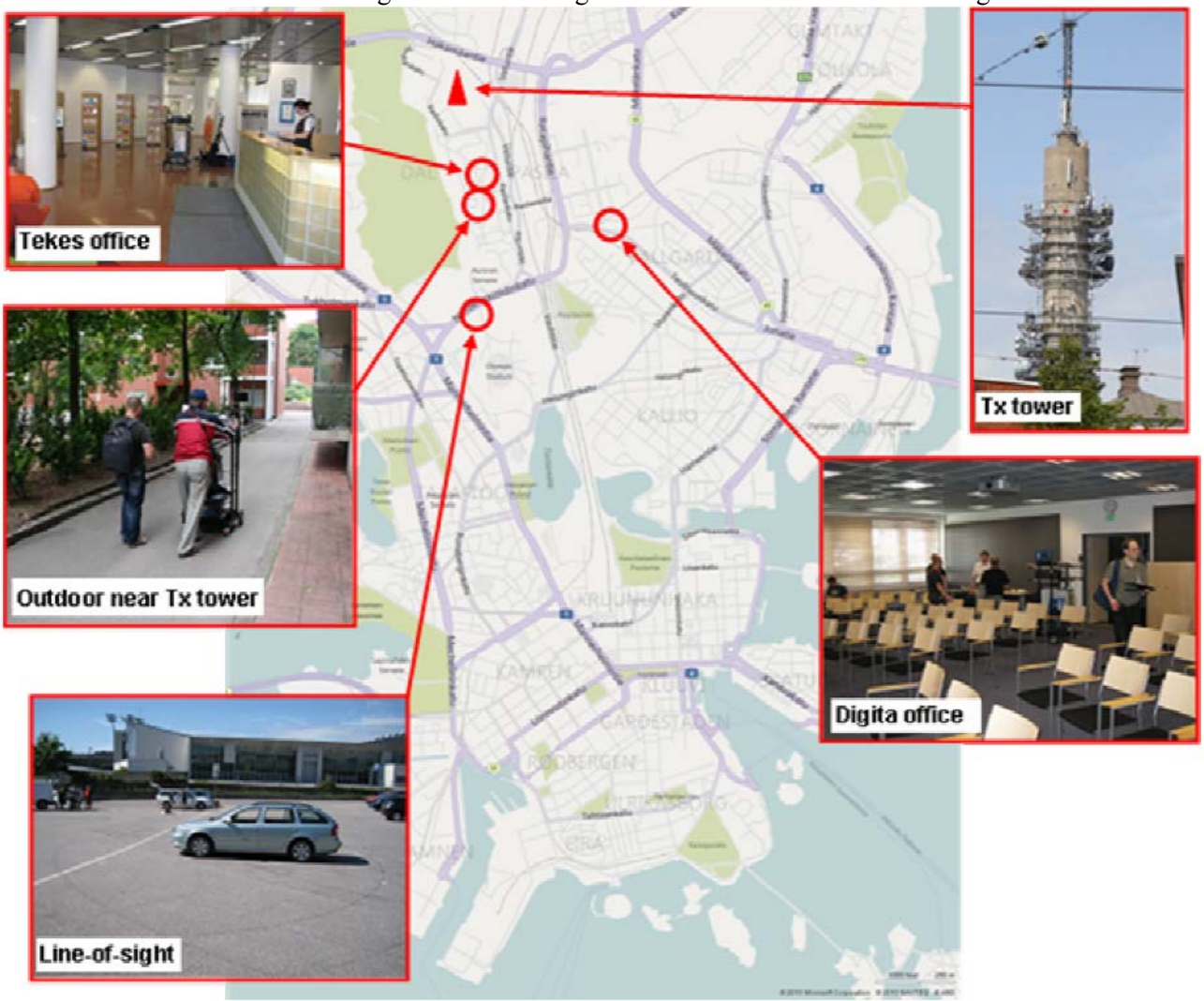


**Figure 1: Locations where measurements were taken**

## 3.2 Block Diagram Setup

The equipment for the channel sounding was contributed by several partners and the setup can be summarised in the block diagram as shown in Figure 2. The main equipment contributors are as follows:

1. Modulator : BBC R&D
2. Power Amplifier : Digita Oy
3. Transmit antennas : Digita Oy
4. Application antennas :
    a. Amphenol
    b. BBC
    c. Nokia
    d. TUAS (x2)
5. Channel Recorder (data capture) : Elektrobit
6. MIMO Receiver (channel display) : BBC R&D

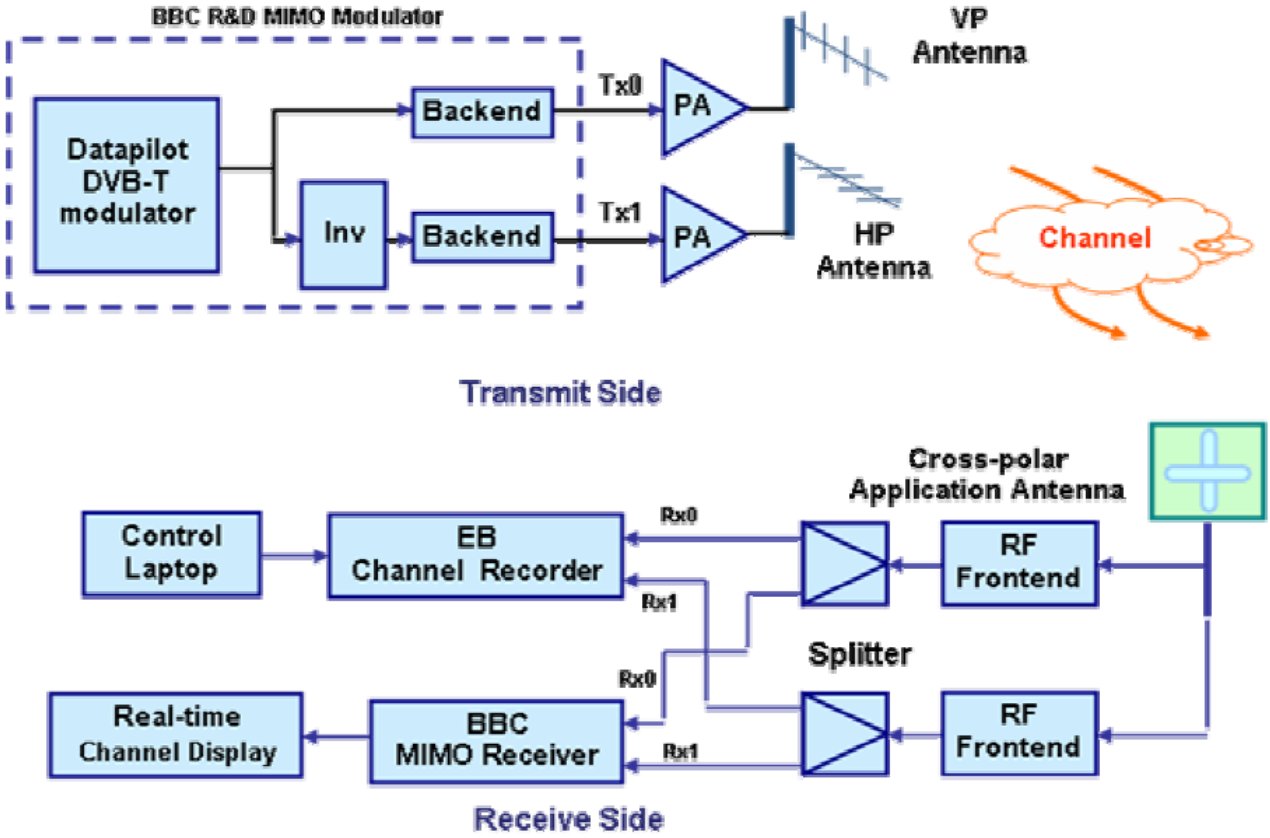


**Figure 2: Block diagram of channel sounding setup**

## 3.3 Application Antennas

Five application antennas (referred to APP1, APP2, APP3, APP4 and APP5 during the campaign) were used with Elektrobit's data capture receiver to record the channel. These antennas were provided by Amphenol, Nokia, TUAS and BBC as stated earlier.

## 3.4 Transmitter

The Pasila Tower was used to transmit the data pilots in both the horizontal and vertical polarized plane. It is situated at the north of the city as indicated in Figure 1. The horizontal and vertical antennas mounted on the transmitting tower are shown in Figure 3. This transmitting tower is approximately 146m above ground level with the technical equipment located at the height of 112m.

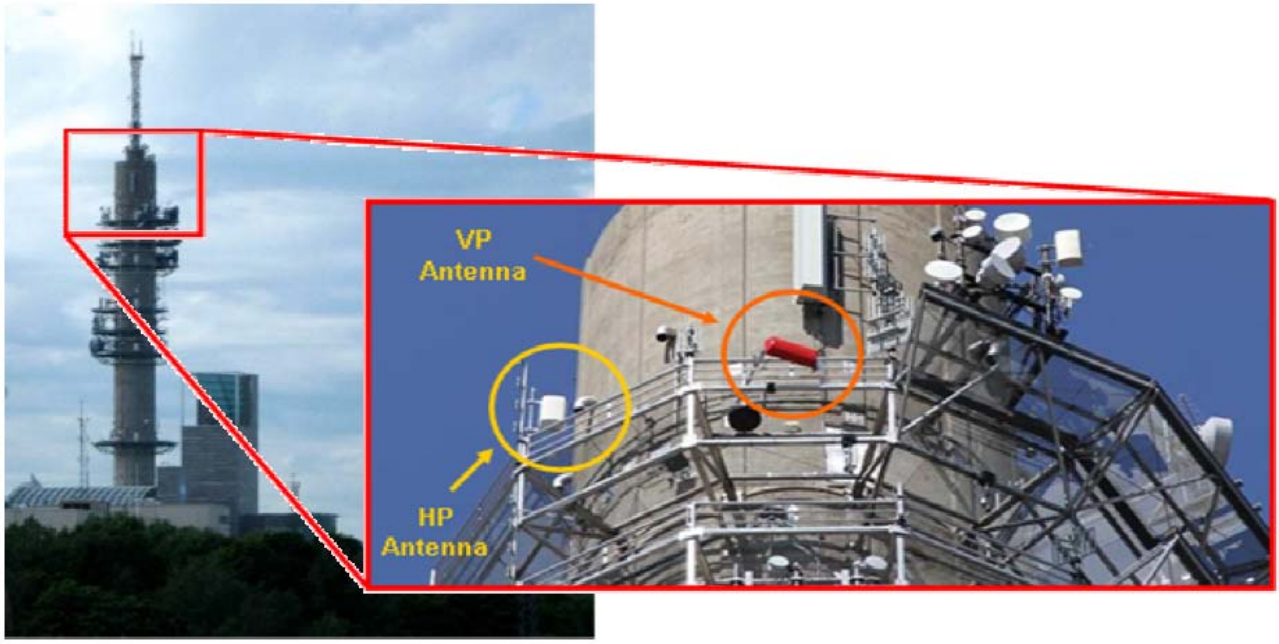


**Figure 3: Transmitter tower (Pasila)**

## 3.5 Modulator

The modulator's firmware has been programmed to output pilot data as described in the signal chapter 2. This system is basically based on DVB-T specification with the data carriers modulated in a predefined long PRBS sequence. The PRBS has a sequence length of $2^{23}$-1 with the generator polynomial $X^{23}+X^{18}+1$. The equipment setup inside the transmitting tower is shown in Figure 4. The output of the power amplifiers were checked to ensure equal power output. It was recorded during the campaign that the output power from the amplifiers are +41.6 dBm.

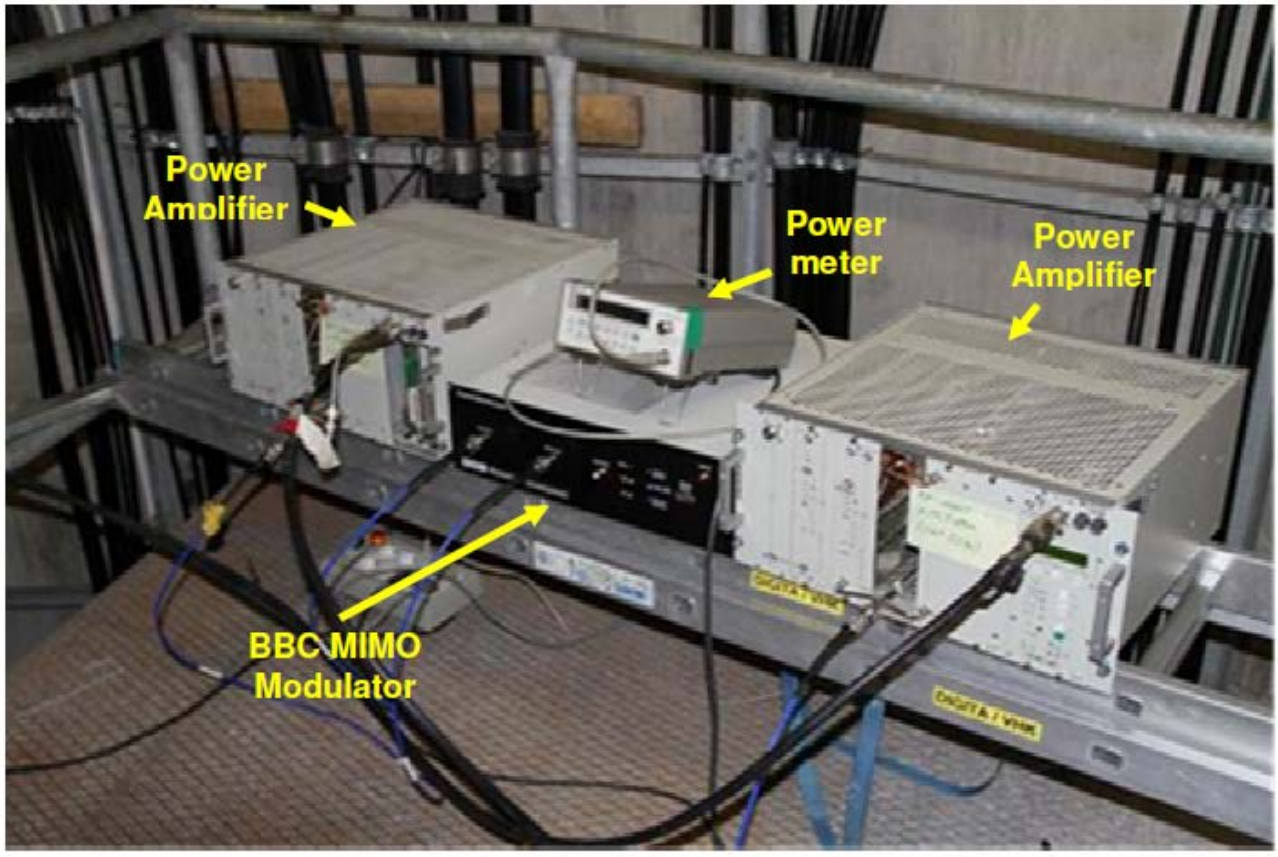


**Figure 4: Modulator setup inside the transmitting tower**

## 3.6 Coverage prediction

The individual coverage prediction for the horizontal and vertical antennas at 1.5m above ground is shown in Figure 5. The horizontal panel antenna was able to cover all the locations specified in this sounding campaign, however the vertical antenna has a much narrower beam-width and hence a panning mechanism was built into the VP antenna setup.

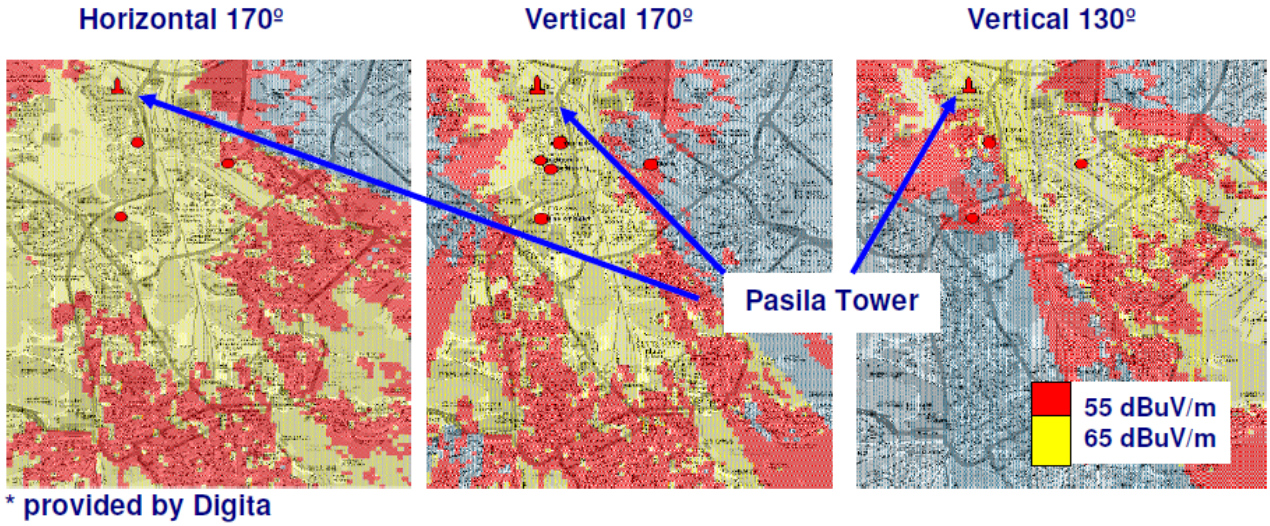


**Figure 5: Coverage prediction on both the horizontal and vertical antennas**

## 3.7 Portable Receiver (for data capture)

The portable receiving station was put together as shown in Figure 6 and it consists of the Elektrobit channel recorder (connected to the control laptop), BBC MIMO receiver with real-time channel display, cross-polar

application antenna and batteries to power up all the equipment. All these were mounted on a push trolley and the application antenna was mounted on an 'extended-arm' to minimize interference from the equipment. The antenna was about 1.5 meters above ground. The real-time channel display was very useful to give an instant feedback of the channel response and to ensure the integrity of the captured data.

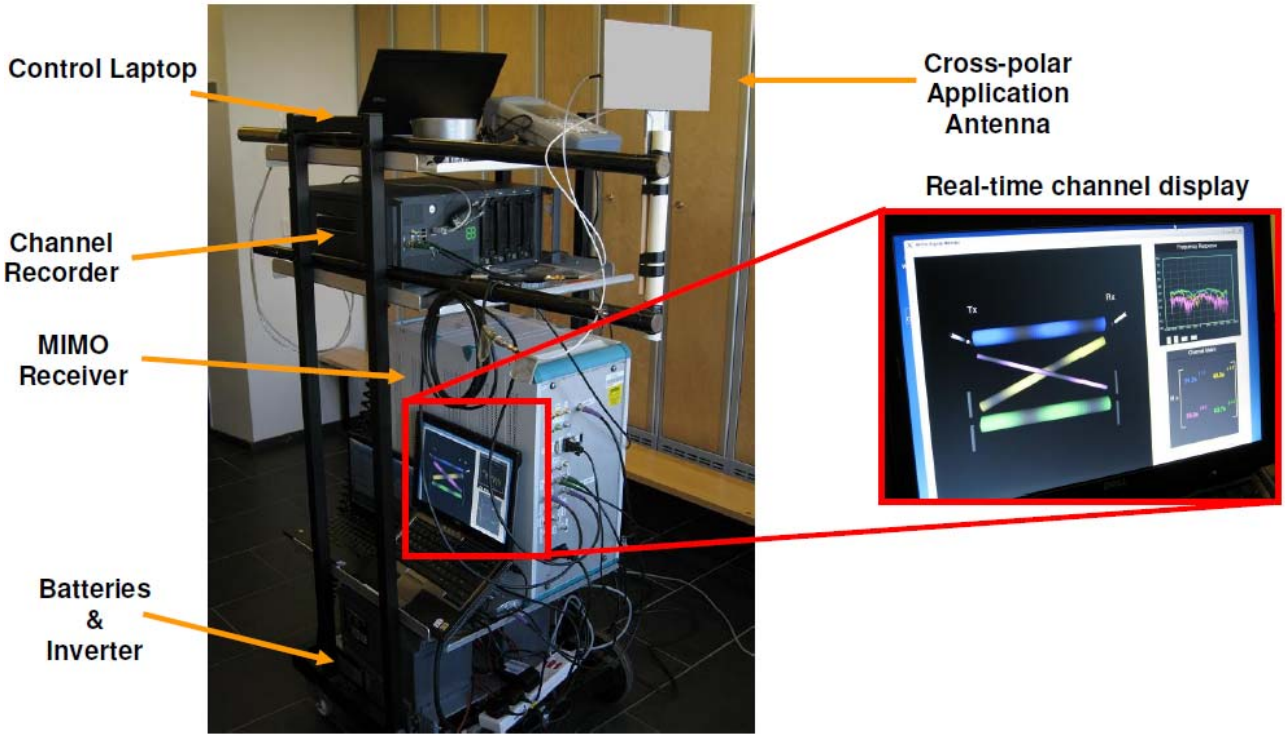


**Figure 6: Portable receiving station**

## 3.8 Campaign Schedule

The channel sounding campaign schedule is as follow:

- Day 1 (28th June 2010)
  - Sounding campaign planning
  - Equipment setup and check
  - Rebuilding of real-time receiver
  - Basic setup test inside Digita office
- Day 2 (29th June 2010)
  - Real measurement recording in Digita office
  - Measurement outside Digita office
- Day 3 (30th June 2010)
  - Calibration
  - Measurement at Olympic stadium car park
  - Indoor & outdoor measurement at the Tekes office
- Day 4 (1st July 2010)
  - Strong non-line-of-sight (NLOS) outdoor measurement near Pasila tower / Tekes office
  - Dismantling setup
- Day 5 (2nd July 2010)
  - Packing and calibration by Elektrobit

At every location, the data capture receiver will follow a specified route where it was repeated with all the five application antennas. At every location, a 6th run was done with the first application antenna mounted in order to check if there are any anomalies during the measurement runs.

## 3.9 Channel models

After collecting all the sounding data, the BBC R&D was heavily involved in processing the data to create the necessary channel models for DVB-NGH. Electrobit, Digita and Tampere University assisted in the initial stages of post-processing while Technische Universität Braunschweig (TU-BS) provided valuable input to the refinement and validation of the channel model. There are also other contributors from the TM-H group in the final Helsinki2 Channel Models document [2].

After analysing all the data, it was proposed that there will be two channel models; Portable Indoor (PI) and Portable Outdoor (PO), for the MIMO configuration in DVB-NGH. The full description of the channel models proposed will be presented in the next chapter.

# 4 DEFINED CHANNEL MODELS (DVB-NGH CHANNEL MODELS)

This chapter describes the channel models which are intended to be used in the development process of the DVB-NGH digital broadcasting standard. The models are created on the basis of the measurements presented here. The text presented here is Complied by Peter Moss (BBC). Contributions to the material are made by Mihail Petrov, Joerg Robert, Pekka Talmola, Erik Stare, Volker Pauli, Danish Nisar, Ismael Gutierrez, Alain Mourad and Peter Moss

The target is to give common definitions of channel models for all who will use them in simulations and laboratory measurements. A variety of models are included to cover a wide range of reception conditions. Also included are specific channel definitions for testing receiver synchronisation issues in SFN-conditions.

The models are intended to be representative of UHF band reception (approximately 500-1000MHz).

The MIMO section of this chapter includes revisions resulting from the 2010 Helsinki channel sounding campaign.

## 4.1 Single-Input-Single-Output (SISO) Channel models

### 4.1.1 Stationary reception

#### Gaussian channel

In this channel model only white Gaussian noise (AWGN) is added to the signal, and there is only one time-invariant path.

#### Simple two path profile, 0dB echo

This profile only includes two paths. Each path, '*i*', is defined by $\alpha_i$, $\tau_i$, $\Delta f_i$ which denote the amplitude, delay and frequency shift of the particular path '*i*', respectively. The profile parameters are given in Table 1.

**Table 1: 0 dB Echo profile**

| i | $\alpha_i$ (dB) | $\tau_i$ (μs) | $\Delta f_i$ (Hz) |
|---|---|---|---|
| 1 | 0 | 0 | 0 |
| 2 | 0 | 0.9Δ | 1 |

For a system based on COFDM with a guard interval, the parameter 'Δ' denotes the guard interval duration in μs. For other systems, it is the stated maximum delay tolerance of the system.

### 4.1.2 Portable reception

#### MIMO-model based

For simulation of portable SISO reception, the path $h_{11}$ taken from the MIMO portable channel definitions shall be used.

### 4.1.3 Mobile Reception

Two SISO models are defined, one based on the MIMO model described below and the other based on the TU6 model

#### MIMO-model based

In this case mobile SISO reception is defined as the path $h_{11}$ taken from the MIMO mobile channel.

#### TU6 Model

This profile reproduces the terrestrial propagation in an urban area. It has been defined by COST 207 as a typical urban (TU6) profile and is made of 6 paths having wide dispersion in delay and relatively strong power. The profile parameters are given in Table 2.

**Table 2: Typical Urban profile (TU6)**

| Tap number | Delay (μs) | Power (dB) | Doppler Spectrum |
|---|---|---|---|
| 1 | 0.0 | -3 | Classical |
| 2 | 0.2 | 0 | Classical |
| 3 | 0.5 | -2 | Classical |
| 4 | 1.6 | -6 | Classical |
| 5 | 2.3 | -8 | Classical |
| 6 | 5.0 | -10 | Classical |

where the Classical Doppler spectrum is defined as:

$$K(f; f_D) = \frac{1}{\sqrt{1-(f/f_D)^2}}$$

The Doppler width parameter should be assigned values corresponding to 60km/h and 350km/h at 600MHz; i.e. **33.3Hz** and **194.8Hz**.

## Mobile TU6-based SFN

This profile reproduces the terrestrial propagation in an urban area in a Single Frequency Network (SFN). Each transmitter in the SFN is modelled as one independent TU6 profile and the total Mobile SFN channel is therefore the sum of all individual and independent TU6 channel models, each having a unique level and delay. A frequency shift shall also be introduced in each test path as detailed below.

One particular TU6 profile, i.e. the received paths originating from one particular transmitter, is denoted $\alpha_i TU6(\tau_i)$, where $\alpha_i$ and $\tau_i$ are the amplification and delay constants to be applied to all individual paths of that particular TU6 profile. In the special case with only one transmitter the values of $\alpha_i$ and $\tau_1$ are set to unity and zero respectively.

The general mobile SFN channel profile, SFN-TU6, with N transmitters can be described in the following way:

$$\text{SFN-TU6} = \sum_{i=1}^{N} \alpha_i TU6(\tau_i)$$

In a real SFN almost any values of $\alpha_i$ and $\tau_i$ may appear, $\tau_i$ values however being limited by the size of the SFN. Also the value of N may vary a lot depending on SFN, although the actual number of transmitters to be considered in the channel profile modelling may depend on the particular network design and receiver performance.

Important special cases of this general model are the cases with two or three transmitters, i.e. the cases N=2 and N=3 with wide variations of $\alpha_i$ and $\tau_i$ values. In case of "classical OFDM" the parameter Δ denotes the guard interval length; in a non-OFDM system it would correspond to the specified maximum delay tolerance of the system.

### Two transmitter test profile (N=2)

$\tau_1$ = 0 μs, $\tau_2$ ={0.05Δ 0.9Δ} $\Delta f_1$=0 $\Delta f_2$=+2Hz

$\alpha_1$ = 0 dB, $\alpha_2$ = {0, -3, -6, -9} dB ("post echo" case)

$\alpha_2$ = 0 dB, $\alpha_1$ = {0, -3, -6, -9} dB ("pre echo" case)

### Three transmitter test profile (N=3)

$\Delta f_1$=0 $\Delta f_2$=+2Hz $\Delta f_3$=-2Hz

1st TU6 ("Pre echo")

$\alpha_1$ = {0, -3, -6, -9} dB

$\tau_1$ = -0.45Δ

2nd TU6 ("Main signal")

$\alpha_2$ = 0 dB

$\tau_2$ = 0 μs

3rd TU6 ("Post echo")

$\tau_3$ = 0.45Δ

$\alpha_3$ = {0, -3, -6, -9} dB

Note: $\alpha_1$ and $\alpha_3$ values to be varied independently.

## 4.2 Multiple-Input-Multiple-Output (MIMO) Channel models

### 4.2.1 General approach

The aim is to provide a time-domain model of paths shown as $h_{11}, h_{12}, h_{21}, h_{22}$ in the figure below, where Tx1 and Tx2 represent a cross-polar pair of antennas at a terrestrial transmitter site and Rx1 and Rx2 the two elements of a MIMO receive antenna whether fixed or mobile.

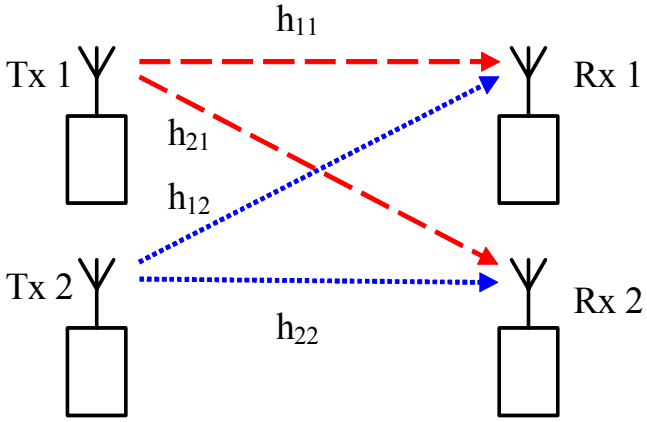


**Figure 7: 2-by-2 MIMO system**

The two proposed models, outdoor portable and indoor portable, will now be described.

### 4.2.2 Outdoor portable model

An 8-tap model of the propagation paths is proposed. The delays and relative power gains of the direct paths $h_{11}, h_{22}$ are tabulated below in Table 1. Taken together with the cross-polar terms $h_{12}, h_{21}$ the sum of the tap powers is unity (0dB).

**Table 3: Power delay profile of the 8-tap outdoor model.**

| **Tap number, *p*** | **Excess delay, $\tau_p$ (μs)** | **Co-polar power gain $\sigma_{11(\tau_p)}^2 = \sigma_{22(\tau_p)}^2$ (dB)** |
|---|---|---|
| 1 | 0 | -4.0 |
| 2 | 0.1094 | -7.5 |
| 3 | 0.2188 | -9.5 |
| 4 | 0.6094 | -11 |
| 5 | 1.109 | -15 |
| 6 | 2.109 | -26 |
| 7 | 4.109 | -30 |
| 8 | 8.109 | -30 |

When used in a discrete baseband model, the excess delays will be rounded to integer sample periods. For instance, in the case of an 8 MHz bandwidth the sample period T is 7/64 us and the resulting discrete excess delays are 0, 1, 2, 6, 10, 19, 38, and 74 samples.

The cross-polar discrimination (XPD) is defined as the ratio of the co-polarized average received power to the cross-polarized average received power. XPD quantifies the separation between the two cross-polarized channels. The larger the XPD, the less energy is coupled between the cross-polarized channels.

The XPD for outdoor and indoor reception takes the following values:

**Table 4: Cross-polar discrimination for outdoor reception.**

| **Environment** | ***XPD* (linear scale)** | ***XPD* (log scale)** |
|---|---|---|
| Outdoor | 4 | 6 dB |

The reciprocal XPD factor $w^2$ for tap $p$ is defined as $w^2 = \sigma_{12}^2(\tau_p)/\sigma_{11}^2(\tau_p) = \sigma_{21}^2(\tau_p)/\sigma_{22}^2(\tau_p)$.

The time-variant channel model for the link between TX antenna $n$ and RX antenna $m$ can be written as:

$$h_{mn}(t,\tau) = \sum_{p=1}^{N_p} g_{mn}(t,\tau_p)\delta(\tau-\tau_p) \qquad (2)$$

Where $t$ is time index, $\tau$ the delay index, $N_p$ (= 8) the number of paths, $\tau_p$ the $p$-th excess delay ($\tau_1$ = 0), and $g_{mn}(\tau_p,t)$ the $p$-th time-variant complex-valued gain.

A 2x2 time-variant matrix **H** is then defined as:

$$\mathbf{H}(t,\tau) = \begin{bmatrix} h_{11}(t,\tau) & h_{12}(t,\tau) \\ h_{21}(t,\tau) & h_{22}(t,\tau) \end{bmatrix} \qquad (3)$$

## Outdoor portable parameters

In the outdoor portable environment, the XPD is 4, as tabulated in Table 4.

For the **first tap** $\tau_1$, the complex-valued gain is purely LOS:

$$g_{mn}(t,\tau_1) = [\sigma_{mn}(\tau_1)\exp(j\theta_{mn})]\ldots(m=n) \quad (4A)$$

$$g_{12}(t,\tau_1) = [\sigma_{12}(\tau_1)\exp(j(\theta_{12}+4\pi t))] \quad (4B)$$

$$g_{21}(t,\tau_1) = [\sigma_{21}(\tau_1)\exp(j(\theta_{21}-4\pi t))] \quad (4C)$$

- The overall K-factor of the outdoor model ($K_0$) is 1.0
- $\theta_{mn}$ are the initial phases of the LOS component. They are real-valued i.i.d. random variables uniformly distributed in the interval [0, 2π). The LOS components of the direct terms ($n$=$m$) have no Doppler shift, whereas for cross-terms a shift of ±2Hz is specified.
- $w^2 = 0.25$

For the **remaining taps** ($p$ = 2…8), only NLOS component is assumed, as expressed below:

$$g_{mn}(t,\tau_p) = \varphi_{pmn}(t) \quad (5)$$

- $w^2 = 0.25$
- $\varphi_{pmn}(t)$ are the time-variant random components of the tap, which model the Doppler spread. They are complex-valued zero-mean Gaussian processes having a combination of a Jakes spectrum and a fixed frequency offset and exhibiting intra-tap correlation. The vector $\varphi_p(t) = [\varphi_{p11}(t) \quad \varphi_{p12}(t) \quad \varphi_{p21}(t) \quad \varphi_{p22}(t)]^T$ is specified to have the following covariance matrix at the $p^{th}$ tap:

$$\mathbf{R}_p = \sigma_{11}^2(\tau_p)\begin{pmatrix} 1.00 & 0.06 & 0.06 & 0.05 \\ 0.06 & 0.25 & 0.03 & 0.05 \\ 0.06 & 0.03 & 0.25 & 0.06 \\ 0.05 & 0.05 & 0.06 & 1.00 \end{pmatrix} \quad (6)$$

The Cholesky decomposition can be used to provide a transition matrix to pre-multiply a 4-element i.i.d. vector at each tap to create the above autocorrelation properties. A suitable matrix is

$$\mathbf{V} = \begin{pmatrix} 1.00 & 0 & 0 & 0 \\ 0.06 & 0.4964 & 0 & 0 \\ 0.06 & 0.0532 & 0.4935 & 0 \\ 0.05 & 0.0947 & 0.1053 & 0.9887 \end{pmatrix} \quad (7)$$

N.B. Using the matrix **V** does not remove the need for the term $\sigma_{11}^2(\tau_p)$

The Jakes spectrum $S(f, f_d)$ is characterized by the following equation:

$$S(f, f_d) = \frac{1}{\pi f_d \sqrt{1-\left(\frac{f}{f_d}\right)^2}} \quad \forall f \in ]-f_d, f_d[; \quad = 0 \quad \text{elsewhere} \tag{8}$$

Where $f_d$ is the maximum Doppler frequency, which is chosen to be proportional to an assumed vehicle speed $v$. In (8), $f_d$ is strictly greater than 0.

The typical receiver velocities we consider for outdoor portable reception are **0km/h** and **3 km/h**. At a carrier frequency of 600 MHz the resulting Doppler frequency $f_d$ is **1.67 Hz**.

The spectrum of the $p^{th}$ tap is shown in the table below:

**Table 3: Tap spectral characteristics of the 8-tap outdoor model.**

| **Tap number, *p*** | |
|---|---|
| 1 | LOS only, no additional Doppler shift |
| 2 | $S\left(f-\frac{3f_d}{4}, \frac{f_d}{4}\right)$ |
| 3 | $S\left(f-\frac{3f_d}{4}, \frac{f_d}{4}\right)$ |
| 4 | $S\left(f+\frac{3f_d}{4}, \frac{f_d}{4}\right)$ |
| 5 | $S\left(f+\frac{3f_d}{4}, \frac{f_d}{4}\right)$ |
| 6 | $S\left(f+\frac{3f_d}{4}, \frac{f_d}{4}\right)$ |
| 7 | $S\left(f+\frac{3f_d}{4}, \frac{f_d}{4}\right)$ |
| 8 | $S\left(f+\frac{3f_d}{4}, \frac{f_d}{4}\right)$ |

### 4.2.3 Indoor portable model

An 8-tap model of the propagation paths is again proposed. The delays and relative power gains of direct paths $h_{11}, h_{22}$ are tabulated below in Table 4. Taken together with the cross-polar terms $h_{12}, h_{21}$ the sum of the powers is unity (0dB).

**Table 4: Power delay profile of the 8-tap indoor model.**

| **Tap number, *p*** | **Excess delay, $\tau_p$ (μs)** | **Co-polar power gain $\sigma_{11}^2 = \sigma_{22}^2$ (dB)** |
|---|---|---|
| 1 | 0 | -6.0 |
| 2 | 0.1094 | -8.0 |
| 3 | 0.2188 | -10 |
| 4 | 0.6094 | -11 |
| 5 | 1.109 | -16 |
| 6 | 2.109 | -20 |
| 7 | 4.109 | -20 |
| 8 | 8.109 | -26 |

The XPD for outdoor and indoor reception takes the following values:

**Table 5: Cross-polar discrimination for outdoor reception.**

| **Environment** | ***XPD* (linear scale)** | ***XPD* (log scale)** |
|---|---|---|
| Indoor | 1.78 | 2.5 dB |

### Indoor portable parameters

For the **first tap** $\tau_1$, the complex-valued gain is split into two components, LOS and NLOS. This writes as:

$$g_{mn}(t,\tau_1) = \left[ \underbrace{\sigma_{mn}(\tau_1)\sqrt{\frac{K}{1+K}}\exp(j\theta_{mn})}_{LOS} + \underbrace{\sqrt{\frac{1}{1+K}}\varphi_{1mn}(t)}_{NLOS} \right] \ldots (m=n) \qquad (4A)$$

$$g_{12}(t,\tau_1)=\left[\underbrace{\sigma_{12}(\tau_1)\sqrt{\frac{K}{1+K}}\exp(j\theta_{12})}_{LOS}\exp(j4\pi t)+\underbrace{\sqrt{\frac{1}{1+K}}\varphi_{112}(t)}_{NLOS}\right] \quad (4B)$$

$$g_{21}(t,\tau_1)=\left[\underbrace{\sigma_{21}(\tau_1)\sqrt{\frac{K}{1+K}}\exp(j\theta_{21})}_{LOS}\exp(-j4\pi t)+\underbrace{\sqrt{\frac{1}{1+K}}\varphi_{121}(t)}_{NLOS}\right] \quad (4C)$$

- The overall K-factor of the indoor model ($K_0$) is approximately 0.2
- K, the Ricean-K factor for the first tap is 1
- $w^2 = 0.56$
- Note that $\varphi_{pmn}(t)$ exists in the indoor model for p=1 as well as p=2-8.

The indoor covariance matrices (for taps 2-8 and the NLOS part of tap 1) are defined as

$$\mathbf{R}_p=\sigma_{11}^2(\tau_p)\begin{pmatrix}1.00 & 0.15 & 0.10 & 0.15\\ 0.15 & 0.56 & 0.06 & 0.04\\ 0.10 & 0.06 & 0.56 & 0.15\\ 0.15 & 0.04 & 0.15 & 1.00\end{pmatrix} \quad (9)$$

A suitable transition matrix for the indoor case is

$$\mathbf{V}=\begin{pmatrix}1.00 & 0 & 0 & 0\\ 0.15 & 0.7331 & 0 & 0\\ 0.10 & 0.0614 & 0.7391 & 0\\ 0.15 & 0.0239 & 0.1807 & 0.9717\end{pmatrix} \quad (10)$$

The typical receiver velocities we consider for indoor portable reception are **0km/h** and **3 km/h**. At a carrier frequency of 600 MHz the resulting Doppler frequency $f_d$ is **1.67 Hz**.

The spectrum of the $p^{th}$ tap is shown in the table below:

**Table 6: Tap spectral characteristics of the 8-tap indoor model.**

| **Tap number, *p*** | |
|---|---|
| 1 (NLOS component) | $S(f, f_d)$ |
| 2 | $S\left(f - \frac{3f_d}{4}, \frac{f_d}{4}\right)$ |
| 3 | $S\left(f - \frac{3f_d}{4}, \frac{f_d}{4}\right)$ |
| 4 | $S\left(f + \frac{3f_d}{4}, \frac{f_d}{4}\right)$ |
| 5 | $S\left(f + \frac{3f_d}{4}, \frac{f_d}{4}\right)$ |
| 6 | $S\left(f + \frac{3f_d}{4}, \frac{f_d}{4}\right)$ |
| 7 | $S\left(f + \frac{3f_d}{4}, \frac{f_d}{4}\right)$ |
| 8 | $S\left(f + \frac{3f_d}{4}, \frac{f_d}{4}\right)$ |

### 4.2.4 Additional antenna rotation and asymmetry terms

The following applies to both outdoor and indoor models.
In deriving the antenna-specific data from which the model parameters were derived, the raw data was rotated by up to ±40º to find the angle which maximised the cross-polar discrimination. This was to correct for both physical mounting differences and antenna axis differences with respect to the casing. It also ensured averaging across antennas retained legitimacy in terms of cross-polar discrimination.

However in practice this 'ideal' alignment may not be representative and so a further rotation matrix **W**, with angle Ω chosen from the set {-45 º, 0 º, +45 º} is recommended with the angle fixed for a particular simulation run.
In addition, an asymmetry matrix **Γ** is included to model observed H/V asymmetries which persist over many contiguous channel realisations (typically over 10m). **Γ** should also be taken as fixed for a particular simulation run. It takes values from the set

$$\left\{\begin{bmatrix} 1.1074 & 0 \\ 0 & 0.8796 \end{bmatrix} \begin{bmatrix} 1 & 0 \\ 0 & 1 \end{bmatrix} \begin{bmatrix} 0.8796 & 0 \\ 0 & 1.1074 \end{bmatrix}\right\}.$$

The resulting channel matrix $\mathbf{H}_c(t,\tau)$ is hence derived from $\mathbf{H}(t,\tau)$ as follows:

$$\mathbf{H}_c(t,\tau) = \mathbf{W}\mathbf{H}(t,\tau)\mathbf{\Gamma} = \begin{bmatrix} \cos\Omega & -\sin\Omega \\ \sin\Omega & \cos\Omega \end{bmatrix} \begin{bmatrix} h_{11}(t,\tau) & h_{12}(t,\tau) \\ h_{21}(t,\tau) & h_{22}(t,\tau) \end{bmatrix} \begin{bmatrix} \Gamma_{11} & 0 \\ 0 & \Gamma_{22} \end{bmatrix} \quad (11)$$

### 4.2.5 Simulation practicalities

#### Updating LOS phases, W and Γ

The LOS phases $\theta_{mn}$ and parameters **W** and **Γ** are both intended to be fixed for periods of five seconds before re-initialisation. This can be relaxed if the time-interleaving length of the system is considerably shorter than this such that no material change in the results would be expected. Indeed, re-initialising per TI frame is acceptable if it is clear this is equivalent to the longer runs. Sudden changes of parameters during OFDM blocks should be avoided however.

Furthermore, regarding matrix **W**, if it is clear that the angles +45º and -45 º give the same result in a particular scheme, the requirement to do both can be dropped.

### 4.2.6 Generating fixed channel realizations (0Hz Doppler snapshots)

If we simulate a time-invariant channel, i.e. $f_d$ = 0, the Doppler shift for the LOS components and the Doppler spreads for the NLOS components are not modelled. Instead, it suffices to generate a number of independent realizations.

For each LOS component we generate four real-valued i.i.d. phases $\theta_{mn}$ with uniform distribution. For the NLOS components we need to generate four complex-valued variables $\varphi_{pmn}$ with the prescribed intra-tap correlation properties.

### 4.2.7 Mobile vehicular outdoor model

For the mobile case, we use the outdoor model and consider two receiver velocities: **60 km/h** and **350 km/h**. At a carrier frequency of 600 MHz the resulting Doppler frequencies $f_d$ are **33.3 Hz** and **194.8 Hz** respectively.

### 4.2.8 4 x 2 model (& 2-tower SFN)

A pair of uncorrelated 2 x 2 models should be invoked, one of which has a time offset taken from {0.05Δ, 0.9Δ}

where Δ denotes the guard interval length for an OFDM system. In a non-OFDM system it would correspond to the specified maximum delay tolerance of the system.

The time-shifted element should additionally have a fixed frequency offset of +1.0Hz.

A second parameter is the power ratio between the signals received from the two towers, which models the power imbalance. Suggested values are {0, -3, -6, -9} dB.

## 4.3 SISO, MISO and SIMO systems

Appropriate transmission paths of the MIMO model may be selected to provide SISO, MISO and SIMO models.

# 5 REFERENCES

[1] ETSI EN 300 744 V1.4.1 (2001-01) : Digital Video Broadcasting (DVB); Framing structure, channel coding and modulation for digital terrestrial television

[2] TM-NGH063r5_DVB-NGH_Helsinki2_channel _models_1v5.pdf